



ELSEVIER

Journal of Chromatography A 822 (1998) 125–136

JOURNAL OF
CHROMATOGRAPHY A

Selection and optimization of background electrolytes for simultaneous detection of small cations and organic acids by capillary electrophoresis with indirect photometry

Xiang Xiong^a, Sam F.Y. Li^{a,b,*}

^aDepartment of Chemistry, National University of Singapore, 10 Kent Ridge Crescent, Singapore 119260, Singapore

^bInstitute of Materials Research and Engineering, National University of Singapore, 10 Kent Ridge Crescent, Singapore 119260, Singapore

Received 17 February 1998; received in revised form 23 June 1998; accepted 3 July 1998

Abstract

Background electrolytes (BGEs) containing two UV-absorbing probes were designed to separate and detect alkali metals and organic acids simultaneously. Imidazole, 1,2-dimethylimidazole, benzylamine, sulfosalicylic acid, trimellitic acid, and pyromellitic acid were tested as the cationic and anionic components of the BGE. By comparing the electrophoretic behavior and UV absorption characteristics of these compounds, it was found that the 1,2-dimethylimidazole/trimellitic acid combination was the most suitable BGE for the separation of alkali metals and organic acids. 18-Crown-6, added as an organic additive for resolving NH_4^+ and K^+ peaks, had no influence on the separation and detection of the organic acids. Separation conditions were optimized by using a three-factor, three-level, face-centred central composite design with respect to three individual (electroosmotic flow, analysis time, and separation quality) and combined responses. The results obtained showed that proper selection of the BGEs and separation conditions are essential in the simultaneous detection of small cations and anions. Under optimal conditions, NH_4^+ , K^+ , Na^+ , Li^+ , ascorbate, sorbate, benzoate, lactate, acetate, succinate, malate, tartarate, maleate, malonate, perchlorate, and oxalate could be separated and detected within 6 min with detection limits ranging from 0.08 to 5 $\mu\text{g}/\text{ml}$. The newly developed method was successfully used to analyze three soft drinks, i.e., apple, orange, and grape juices. The results obtained showed that the present approach was simple, fast and could be applied to the analysis of real samples. © 1998 Elsevier Science B.V. All rights reserved.

Keywords: Background electrolyte composition; Optimization; Soft drinks; Food analysis; Fruit juices; Inorganic cations; Organic acids

1. Introduction

Small cations and organic acids are different classes of analytes. They exist in many samples, such as foods, beverages, cosmetics, drugs, and etc. [1–3].

It is very interesting and useful to separate these two classes of analytes simultaneously, because much more information about the samples and chemical processes would be obtained with less work and a short analysis time.

Simultaneous separation and detection of cations and anions in a single run is not easy in capillary electrophoresis (CE), because these two classes of

*Corresponding author. Tel.: 65-874-2681; Fax: 65-779-1691; E-mail: chmlifys@leonis.nus.sg

analytes tend to migrate in opposite directions under a given electric field. Although several approaches have been developed to deal with this problem, the solution obtained is still far from being satisfactory. The first approach developed for this kind of separation was to use a single detector and a larger electroosmotic flow (EOF) to force the cations and anions to migrate in the same direction towards the detector [4,5]. Only the separation of some large organic molecules/biomolecules and slow moving inorganic anions [6] were demonstrated by using this approach. It seems that this approach is a bit difficult to handle with the simultaneous separation of fast moving cations and anions, because it was not well understood how large the EOF should be to ensure that both the small cations and anions move towards the detector. In order to cope with this problem, Bachmann et al. developed a system by using two detectors and two capillaries without controlling of the EOF to achieve the simultaneous separation of some small cations and chloroanions [7]. Unfortunately, their approach is experimentally complicated and inconvenient. Recently, Kuban and Karlberg reported a system in which the detector was placed at the center of the capillary and the sample was injected from both ends of the capillary [8]. Most of the common small cations and anions were separated in their system, but this approach is experimentally tedious and difficult to exploit on a commercially available CE instrument. The present work reports another approach to separate the small cations and organic acids simultaneously by using the principle of enlarging EOF and one sample injection on a single detector system.

Two problems should be solved for the simultaneous separation and detection of small cations and organic acids by CE. One is the control of the migration direction of these two types of substances so that they can move in the same direction towards the detector. The other is the synchronous detection of them at the detector. Generally, conductometric [9,10] and indirect photometric [11–13] modes are the choices for the detection of these substances because most of them are nonchromophoric. However, the large differences of their conductances make the proper suppression of the signal due to the background electrolyte (BGE) a great challenge to the simultaneous detection of these two classes of

ions by the conductivity mode. The indirect photometric method is the more widely used detection mode and would be employed for the present study.

The conventional BGEs could not be used for the simultaneous determination of these two classes of analytes, because only one chromophoric probe would be involved in the BGEs and their separation conditions are expected to be quite different for these two classes of analytes. This suggests that in order for these two classes of analytes to be determined simultaneously a common separation condition should be found and a new type of BGE should be formulated.

The aim of the present work is to develop a method for simultaneous separation of small cations and organic acids by CE with indirect photometric detection. The main focus is on the strategies of formulation of the binary BGEs and optimization of the separation conditions. A central composite design was used to examine the effects of pH, the concentration of BGEs and the concentration of the organic additive (18-crown-6) on three individual responses (electroosmotic flow, analysis time, and separation quality) and combined responses. Finally, the newly formulated BGE was applied in the analysis of three commercially available soft drinks (apple juice, orange juice and grape juice) under the optimal condition.

2. Experimental section

2.1. Chemicals and solutions

All chemicals used in the present experiments were analytical grade or better. Imidazole (>99.5%), benzylamine (>99%), pyromellitic acid (>97%) were obtained from Fluka (Fluka Chemie, Buchs, Switzerland). Sulfosalicylic acid (A.C.S. reagent) and 1,2-dimethylimidazole (>98%) were purchased from Aldrich (Aldrich, Milwaukee, WI, USA). Trimellitic acid (>99%) was obtained from TCI (Tokyo Chemical Industry, Tokyo, Japan). All solutions were prepared with Millipore water from a Milli-Q system (Millipore, Bedford, MA, USA). The stock solutions of standard analytes were prepared to ca. 1500 µg/ml by dissolving known amounts of each reagent in Millipore water. The model sample mixtures at µg/

ml level were prepared daily by stepwise dilution of the standard stock solutions. The stock electrolyte solutions were prepared to be ca. 20 mM and the working electrolyte solution was prepared by dilution from the stock solution daily.

2.2. Apparatus

A home-made capillary electrophoresis system, which consisted of a MicroUVIS 20 detector (Carlo Erba Instruments, Milan, Italy), a high-voltage power supply (Spellman, Plainview, NY, USA), a DP700 data processor (Carlo Erba Instruments, Milan, Italy), and a fused-silica capillary (Polymicro Technologies, Phoenix, AZ, USA), was used throughout the experiment. The dimensions of the capillary were 50- μm I.D. \times 358- μm O.D. The total length of the capillary was 44.0 cm with an effective length of 38.0 cm. A pH meter (Model HANNA B417, Woonsocket, RI, USA) with ± 0.01 pH resolution was used to measure the pH of the electrolyte solutions throughout the experiment. The UV-Vis spectra were obtained with a HP8452A diode array spectrophotometer (Hewlett-Packard, Waldbronn, Germany).

2.3. Capillary treatment

Each day, before sample injection, the capillary was rinsed with 1 M NaOH for half an hour, and then with 0.1 M NaOH for 15 min, followed by the running electrolyte solution for another half an hour. After that, the capillary was washed by the running electrolyte under working voltage (29.0 kV) for 5–10 min until the baseline became stable. Through these treatments, the capillary was ready for use. No further washing of the capillary was performed in between sample injections unless a noisy baseline was observed. In the case of noisy baseline, the capillary was flushed with the running electrolyte solution for 4 or 5 times of the total volume of the capillary, and then washed by the running electrolyte solution under working voltage for several min until a stable baseline was reached. The results obtained showed that this treatment of capillary provided satisfactory reproducibility of the migration times with 0.7% R.S.D. (with respect to EOF) for triplicate

injections. The capillary was washed daily with water purified with a Millipore-Q system.

2.4. Procedures

All running electrolyte solutions were prepared daily by pipetting a certain volume of the organic base stock solution into a 15-ml bottle. The pH was adjusted with the organic acid to a specific pH value on the pH meter. Then the electrolyte solution was transferred to a 10-ml volumetric flask and diluted with Millipore water to the graduated marker. Prior to use, the running electrolyte solution was filtered through a 0.45- μm membrane filter (Phenomenex, Torrance, CA, USA), and then transferred to the two electrolyte reservoirs for separation. Indirect UV detection was carried out at 210 nm wavelength, unless otherwise stated, with reversal of the polarity of the signal output. The detector was located at the cathodic end of the capillary. Sample injections were performed hydrostatically at the anodic end of the capillary by raising the sample vial 19 cm above the level of the other/waste reservoir for several tens of seconds (see Section 3 for the details). In between sample injections, approximately 30 s of standby time was adopted to minimize cumulative Joule-heating effect.

2.5. Sample treatment

Apple, orange and grape juices were obtained from the local supermarket. No specific treatment of the samples was performed except filtration through 0.45- μm membrane filter (Phenomenex, Torrance, CA, USA) after dilution with Millipore water before injection. The dilution ratio for the samples were 1:25 (apple), 1:80 (orange), and 1:50 (grape), respectively.

2.6. Data treatment

The central composite design and modeling of the responses were performed on a statistical software, Modde, version 3.0 (Umetri B, Umeå, Sweden). The solution of linear equations was carried out using Mathematica, version 2.2 (Walfram Research, Champaign, IL, USA), running on Microsoft Windows, version 3.1.

3. Results and discussion

3.1. Formulation of the binary BGE

3.1.1. Selection of the components of the BGE

The success of indirect photometric detection of the cations and organic acids is dependent upon the proper selection of the BGEs. This means that the components in the BGE should have similar mobility with the analytes of interest and strong UV absorption [14,15]. For these purposes, three organic amines and three aromatic acids were initially tested as the components of the BGE. Their electrophoretic and spectroscopic properties were presented in Table 1. It can be seen that both the cationic and anionic components of the BGEs have UV absorption between 200 and 230 nm, and their migration rates towards the detector (at the cathodic side) follow the sequence: benzylamine > 1,2-dimethylimidazole > imidazole > sulfosalicylic acid > trimellitic acid > pyromellitic acid under the observed conditions. It should be noted that 1,2-dimethylimidazole and benzylamine behave like cations at pH larger than 7.0 and less than their pK_a values; whereas imidazole behaves more or less like a neutral molecule at such pH conditions. (It is probably due to the dissociation of the positively charged imidazole at the pH condition [18], which was roughly 0.7 pH unit larger than the pK_a value of imidazole). This implied that

imidazole could not function as a cationic co-ion at pH higher than its pK_a value. Thus it was ruled out as a candidate of the cationic co-ion because the simultaneous separation of small cations and organic acids would be performed under higher pH conditions. Since 1,2-dimethylimidazole had stronger UV absorption than benzylamine at wavelengths between 200 nm and 230 nm (data not shown here), it was chosen as the cationic component to formulate the binary BGE with the three aromatic acids in the subsequent experiments.

With the electrophoretic and spectroscopic information of the anionic components of the BGEs, we could not decide which of them was better matched with the anionic analytes of interest, especially in the situation of simultaneous detection of the small cations and organic acids. Consequently, each of the combinations of 1,2-dimethylimidazole with the three anionic BGEs was tested using a model sample mixture which contained four small cations and twelve anions (eleven organic acids and one inorganic anion used as internal standard), as shown in Fig. 1. From Fig. 1, we can see that the peak height and peak symmetry are different for the three combinations of the binary BGEs, and their working wavelengths are also different. This indicates that the proper formulation of the electrophoretic media and the selection of the operation conditions are essential in the simultaneous separation of small cations and

Table 1
 pK_a values of the potential components of the BGEs and their relative migration times

Component of BGE	pK_a [16]	Band of UV absorption (nm)	Relative migration time (min) ^a
<i>Cationic</i>			
Imidazole	6.99	200–230	–0.01
1,2-Dimethylimidazole	8.21 [17]	200–240	–0.11
Benzylamine	9.33	200–260	–0.16
<i>Anionic</i>			
Sulfosalicylic acid	2.49 (pK_1)	200–350	+1.89
	12.00 (pK_2)		
Trimellitic acid	2.52 (pK_1)	200–320	+2.67
	3.84 (pK_2)		
	5.20 (pK_3)		
Pyromellitic acid	1.92 (pK_1)	200–330	+4.32
	2.87 (pK_2)		
	4.49 (pK_3)		
	5.63 (pK_4)		

^a Relative migration time = $t_{ion} - t_{neutral\ marker}$; the migration times (t_{ion}) of each BGE were determined in 6.75 mM phosphate buffer, pH = 7.70; $\lambda = 210$ nm; the neutral marker used was benzyl alcohol, other conditions as in Fig. 1.

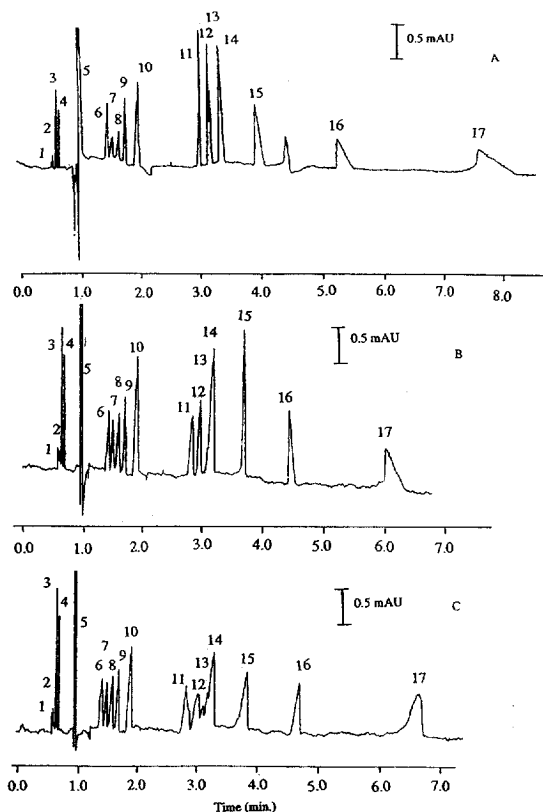


Fig. 1. Separation of four cations and twelve anions in three binary BGEs at pH 7.0. (A) 1,2-Dimethylimidazole (4.0 mM)–sulfosalicylic acid (1.6 mM), $\lambda=217$ nm; (B) 1,2-dimethylimidazole (4.0 mM)–trimellitic acid (1.0 mM), $\lambda=210$ nm; (C) 1,2-dimethylimidazole (5.0 mM)–pyromellitic acid (0.8 mM), $\lambda=210$ nm. 18-Crown-6=2.0 mM in all three binary BGEs; Injection=15 s; other conditions see Section 2; Peak identification ($\mu\text{g/ml}$): 1= NH_4^+ (12.7), 2= K^+ (35.9), 3= Na^+ (173.0), 4= Li^+ (8.7), 5= H_2O , 6=ascorbate (13.3), 7=sorbate (15.5), 8=benzoate (27.5), 9=lactate (10.1), 10=acetate (43.9), 11=succinate (8.4), 12=malate (8.2), 13=tartarate (20.4), 14=malate (8.9), 15=malonate (8.5), 16=perchlorate (8.7), 17=oxalate (6.7).

anions. It should be pointed out that citrate could not be detected in the 1,2-dimethylimidazole–trimellitic acid and 1,2-dimethylimidazole–pyromellitic acid binary BGEs even when the concentration of citrate was increased to 42 $\mu\text{g/ml}$, as shown in Fig. 1B and C, although it could be detected in the 1,2-dimethylimidazole–sulfosalicylic acid binary BGE at the same concentration, as shown in Fig. 1A (the peak in between peak 15 and peak 16 corresponded to citrate). The exact reason is not clear at this

moment. A possible explanation is that the microenvironment around citrate is a lot different for the three BGEs. For simplification, citrate was not included in the model sample mixture in the subsequent experiments. In addition, since NH_4^+ and K^+ have similar electrophoretic behavior, 18-crown-6 was added in the binary BGEs to enhance the resolution of these two components in the model sample mixture.

3.1.2. Selection of detection wavelength

Owing to the fact that two UV-absorbing components were involved in the BGE, the absorbance observed at the detector is the contribution of UV absorption from both of the two components of the BGE, which can be expressed as:

$$A_{\text{obs}}^{\text{B}} = A_{\text{co-ion}}^{\text{B}} + A_{\text{counterion}}^{\text{B}} \quad (1)$$

where A stands for absorbance, and the superscript B represents BGEs (the same in following). After sample injection and separation reached a steady state, the absorbance measured for each of the sample zones at the detector can be expressed as:

$$A_{\text{obs}}^{\text{S}} = A_{\text{co-ion}}^{\text{S}} + A_{\text{sample}}^{\text{S}} + A_{\text{counterion}}^{\text{S}} \quad (2)$$

where S means sample. The differences of the absorptive and electrophoretic characteristics among co-ions, counterions and the samples will result in three observations, namely:

(I) $A_{\text{obs}}^{\text{S}} < A_{\text{obs}}^{\text{B}}$ (normal displacement of the co-ion by the analyte)

(II) $A_{\text{obs}}^{\text{S}} = A_{\text{obs}}^{\text{B}}$ (no peaks detected)

(III) $A_{\text{obs}}^{\text{S}} > A_{\text{obs}}^{\text{B}}$ (positive peaks detected)

This implies that proper selection of the detection wavelength is critical to permit the simultaneous detection of the cations and the anions. Arbitrary selection of the detection wavelength would result in none or positive peaks to be detected. A theoretical explanation of this observation has been detailed by Beckers [19]. Actually, we did observe this phenomenon in the 1,2-dimethylimidazole–sulfosalicylic acid BGE. When the wavelength was not in the region of 214–220 nm, the peaks corresponding to NH_4^+ and K^+ were all positive (i.e. absorbance of

the sample zone was higher than the background). This implied that the absorbances for 1,2-dimethylimidazole and sulfosalicylic acid under a certain pH at the given wavelength region matched well with one another, although the absorbance of sulfosalicylic acid was larger than 1,2-dimethylimidazole at other wavelengths. However, no such phenomena were observed for the other two combinations of the BGEs within the wavelength range of 200–230 nm.

By taking the sensitivity of the detection and peak shapes into consideration for both the cations and the organic acids in the model sample mixture, it was found that the 1,2-dimethylimidazole–trimellitic acid BGE was the best choice for the present work as shown in Fig. 1B. This indicated that the characteristics of the two components of the BGEs could match those of the analytes of interest very well, i.e. in terms of mobility (note the difference in the migration times of the analytes and the neutral marker, water peak, as shown in Table 1) and UV absorption. However, the separation of the cations and organic acids are not satisfactory under the given conditions. Optimization of the separation conditions would be necessary to resolve all the peaks completely.

3.2. Optimization of the separation conditions

3.2.1. Design of experiments

From previous results of our work [20], it was found that the pH, concentration of the cationic BGE, and the separation voltage were the factors effectively affecting the simultaneous separation of small cations and anions. Naturally, the optimization of the separation conditions should be performed on these factors. Moreover, 18-crown-6 was added to resolve K^+ and NH_4^+ in the present separation media, it should also be considered as one of the factors needed to be optimized. In order to reduce the number of experiments and shorten the analysis time as much as possible, separation voltage was fixed at the largest output of the high voltage source used (see Section 2 for the detail). Therefore, the factors involved in the experimental design was pH, concentration of 1,2-dimethylimidazole, and concentration of 18-crown-6. From the results, in the selection of the separation media, it was found that when pH was lower than 6.7, some fast moving

organic acids could not be detected within a reasonable time and the peak shape for these organic acids appeared severely unsymmetrical. However, when pH was higher than pH 8.0, the resolutions for both the cations and the organic acids became poor. As a result, the pH range investigated for the optimization of pH was confined between pH 7.0 and pH 8.0. And the concentration range of 1,2-dimethylimidazole was limited to between 3.0 mM and 4.0 mM. This is because when the concentration of 1,2-dimethylimidazole was lower than 3.0 mM within the pH range mentioned above, the resolutions for the analytes were not acceptable due to the larger EOF produced under these conditions, whereas a noisy baseline was observed when its concentration was higher than 4.3 mM. In addition, it was also found that NH_4^+ and K^+ could be separated to some extent when the concentration of 18-crown-6 was at 2.0 mM, but the separation between them was not achieved when the concentration of 18-crown-6 reached 3.0 mM. This implied that too high a concentration of 18-crown-6 was not beneficial to the separation of NH_4^+ and K^+ in the present case (in contrast to the observation reported in literature [21]). The exact reason is not clear at this moment. One of the possible explanations is that the resolution between NH_4^+ and K^+ is increased by so much, as the concentration of 18-crown-6 was increased to 3.0 mM, that the peak corresponding to K^+ merged with the peak of Na^+ just following it as shown in Fig. 1. Owing to this observation, the concentration range for 18-crown-6 was limited to between 2.0 mM and 3.0 mM. Table 2 (left side) shows the whole experimental domain for all the factors by using a three-factor, three-level, face-centered central composite design. There are 17 runs in total with triplicate runs at the central point (electrolyte solutions 15–17 in Table 2).

3.2.2. Responses and their modeling

The individual responses examined in the present work were electroosmotic flow (EOF), analysis time (represented by the migration time of the last peak, i.e., oxalate peak), and separation quality, which was expressed by the total peak number separated in a single run. The total peak number was obtained by the following protocol:

Table 2

Experimental domain obtained by a three-factor, three-level, face-centred central composite design with the individual and combined responses

Electrolyte solution	pH	1,2-Dimethyl-imidazole (mM)	18-Crown-6 ($10^5 \cdot \text{cm}^2 \cdot \text{V}^{-1} \cdot \text{S}^{-1}$)	EOF ^a (min)	t_i^b	SE _{<i>i</i>} ^c	RF1 ^d (a)	RF2 ^d (b)	RF3 ^d (c)
1	7.0	3.0	2.0	93.3	5.92	13	0.52	0.35	0.70
2	8.0	3.0	2.0	111.7	2.88	10	0.64	0.62	0.65
3	7.0	3.0	3.0	91.5	7.14	14	0.47	0.23	0.70
4	8.0	3.0	3.0	108.0	3.28	10	0.61	0.57	0.64
5	7.0	4.0	2.0	95.1	6.07	13	0.51	0.33	0.69
6	8.0	4.0	2.0	103.3	3.64	11	0.61	0.55	0.67
7	7.0	4.0	3.0	94.2	5.97	13	0.52	0.16	0.69
8	8.0	4.0	3.0	110.5	3.23	11	0.64	0.60	0.69
9	7.0	3.5	2.5	93.3	6.92	14	0.48	0.26	0.71
10	8.0	3.5	2.5	108.0	3.14	11	0.65	0.60	0.69
11	7.5	3.5	2.0	104.4	3.97	13	0.66	0.55	0.76
12	7.5	3.5	3.0	101.1	4.09	14	0.68	0.56	0.81
13	7.5	3.0	2.5	102.2	3.80	13	0.67	0.57	0.77
14	7.5	4.0	2.5	96.1	5.63	15	0.61	0.41	0.80
15	7.5	3.5	2.5	101.1	4.54	14	0.65	0.50	0.79
16	7.5	3.5	2.5	101.1	4.36	14	0.66	0.53	0.80
17	7.5	3.5	2.5	101.1	4.23	14	0.66	0.53	0.80

^a Electroosmotic flow obtained by using Eq. (3) given in Ref. [20].

^b Analysis time represented by the migration time of the last peak (i.e. oxalate).

^c Separation quality in terms of number of peaks obtained by the procedure described in Section 3.2.2.

^d Combined responses obtained by Eq. (3), (a) $Q=U=0.5$; (b) $Q=0.25, U=0.75$; (c) $Q=0.75, U=0.25$.

Step 1. Set an acceptable resolution threshold value (criterion for a complete separation). In the present case, it was preset to be 1.2.

Step 2. Work out the resolution between the adjacent peaks i and $i+1$ starting from the first peak and compare the resolution obtained with the separation criterion. If it is larger or equal to the given resolution, then peak i is counted as a separated peak; otherwise, peak i is not counted as a separated peak.

Step 3. Repeat step 2 one peak forward until the last pair of the adjacent peaks has been checked.

The equations used to work out the separation resolution were described in the literature [22]. After these steps, each electropherogram obtained in the experimental domain was used to calculate a set of individual responses, namely, the EOF, the analysis time (t_i), and the total peak number (SE_i), as given in Table 2 (middle part). These parameters simplify the representation of the separation performance for each of the electropherograms and were considered more explicit than the representation of separation

performance by the sum of resolution of every adjacent peak pairs [23].

A combined response function, which was modified from literature [24] by taking into consideration of the analysis time and separation quality, was designed as below:

$$CRF = QSE_i/SE_{\max} + U(1 - t_i/t_{\max}) \quad (3)$$

Where Q and U are the weighting factors which range from 0 to 1; SE_i and t_i are the total peak number and the analysis time of the i th electropherogram in the experimental domain; SE_{\max} and t_{\max} are the maxima of the total peak number and the analysis time among all the electropherograms. The three typical situations, i.e., (1) analysis time and separation quality have the same significance; (2) analysis time is more significant than separation quality; and (3) analysis time is less significant than separation quality, have been simulated by assuming different weighting factors represented by Q and U . Table 2 (right side) lists all the responses obtained

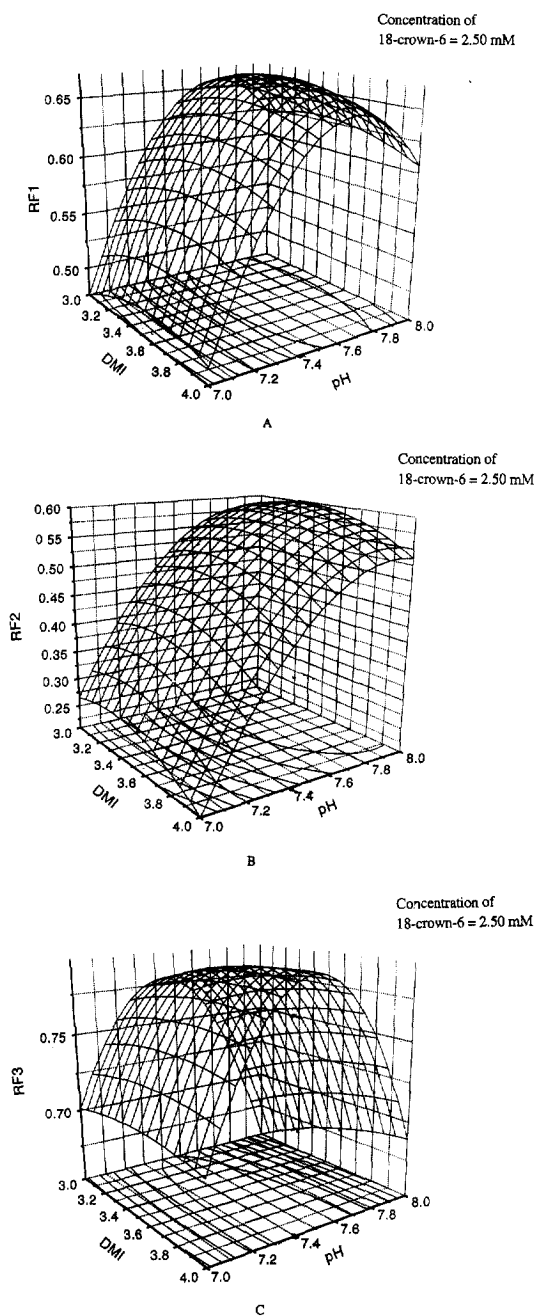


Fig. 2. Three-dimensional plots of the combined responses Eq. (3) against pH and concentration of 1,2-dimethylimidazole (DMI) at the middle level of concentration of 18-crown-6. (A) $Q=U=0.5$; (B) $Q=0.25, U=0.75$; (C) $Q=0.75, U=0.25$.

from each electropherogram in the experimental domain. And they are modeled by using a second-degree polynomial function on the three coded factors as follows:

$$Y = a_0 + a_1X_1 + a_2X_2 + a_3X_3 + a_{11}X_1^2 + a_{22}X_2^2 + a_{33}X_3^2 + a_{12}X_1X_2 + a_{13}X_1X_3 + a_{23}X_2X_3 \quad (4)$$

where Y represents the response; X_1 , X_2 and X_3 represent the coded factors relating to pH, concentration of 18-crown-6, and concentration of 1,2-dimethylimidazole, respectively. They are respectively coded by the following standard equations (Eqs. (5)–(7)), where CR and BA represent the concentrations of 18-crown-6 and 1,2-dimethylimidazole.

$$X_1 = (\text{pH} - 7.5)/0.5 \quad (5)$$

$$X_2 = (\text{CR} - 2.5)/0.5 \quad (6)$$

$$X_3 = (\text{BA} - 3.5)/0.5 \quad (7)$$

The correlation coefficients obtained for each of the responses were larger than 0.93. This indicates that Eq. (4) fits the data very well.

3.2.3. Searching for maxima of the response surfaces

Fig. 2 shows three-dimensional plots of the combined response surfaces and their contour maps. The maxima of the response surfaces were located by differentiating the fitted second-degree polynomial with respect to each factor described previously and equating derivatives to zero. The optimal conditions for the three different situations are given in Table 3. Fig. 3 shows the separation results of the small cations and organic acids under the optimal conditions given in Table 3. It can be seen that all the cations and the organic acids are baseline separated in Fig. 3C.

3.3. Validation of the separation medium

3.3.1. Limits of detection

The limits of detection for all the cations and anions were determined in the optimal condition solution as given in Fig. 3C. The results obtained are shown in Table 4. From this table, we can see that the detection limits for both the cations and the

Table 3
Optimal conditions obtained by using the combined responses at three different situations

	Case 1	Case 2	Case 3
	$Q=U=0.5$	$Q=0.25, U=0.75$	$Q=0.75, U=0.25$
pH	7.68	7.92	7.50
1,2-Dimethylimidazole (mM)	3.48	3.35	4.00
18-Crown-6 (mM)	2.54	2.53	2.86

anions are comparable to those obtained by the individual separation methods [11,12]. This indicated that the developed method had very high sensitivity for the simultaneous detection of the cations and anions. It was noted that the detection limits of the anions were lower than those of the cations as shown in Table 4. The relatively higher detection limits for the cations than those of the anions were probably due to the strong UV absorption of the counterion in the sample zones which masked the decrease of the absorbance caused by the displacement of the cationic co-ion of the BGE by the cations, or it might be that the complexed K^+ by the additive (18-crown-6) decreased the effective displacement of the co-ion when the concentration of K^+ ion was lower than the detection limit. From the practical point of view, the detection limits achieved by the present method are quite acceptable for the analysis of real samples.

3.3.2. Linearity of calibration and reproducibility

In order to evaluate the potential of the present method for quantitative uses, the linearity of the calibration lines were estimated by correlating the peak height to sample concentration. For cations, the concentration ranges of the standard solutions were from at least two times larger than the detection limits upwards to around 30 $\mu\text{g}/\text{ml}$. For anions, the concentration ranges of the individual analytes were from at least four times higher than the detection limits upwards to around 10 $\mu\text{g}/\text{ml}$ and 30 $\mu\text{g}/\text{ml}$. It was found that both the cations and the anions exhibited good linearity within one order of magnitude with correlation coefficients being larger than 0.99. For Na^+ , the linearity of the calibration line was preserved over two orders of magnitude with correlation coefficient being larger than 0.97. However, the linearities of the calibration lines corresponding to ascorbate and lactate were poor in the concentration ranges examined with the correlation

coefficients being 0.82 and 0.84, respectively. The poor linearities of the calibration lines for these anions might be attributed to the mismatch between the mobilities of the co-ions and the analytes. The reproducibility for the peak height ranged from 2% to 8% R.S.D. with triplicate injections. Therefore, it could be concluded that the present method was suitable for the quantitation of the cations and anions simultaneously.

3.3.3. Application

In order to demonstrate the applicability of the developed method, three soft drinks, i.e., apple, orange, and grape juices, were chosen as the test samples. Fig. 4 shows the cations and organic acids separated and identified in these soft drinks under the separation conditions as given in Fig. 3C. From the figure we can see that both the cations and anions of these soft drinks could be determined in a single run within several min. It is very convenient as compared to the individual separation approach by CZE [9,12,25,26], where only the information on either cations or anions could be obtained in a single run. From Fig. 4, we can also see that the concentration distribution of the cations and anions is very wide for the three soft drinks, and the matrix effect in the real samples has strong influence on the migration times of the organic acids, especially citrate, as can be seen in Fig. 4B and C. The influence of the matrix effect might be reflected in the different viscosities of the sample solutions which may affect the electroosmotic flow velocity. It is very interesting to note that citrate could be detected in the real samples, while it could not be detected in the model sample mixture under the same conditions in the same BGE. This observation indicated that the dissociation and association processes between the analyte anions and the free hydrogen ions in the BGE was a dynamic process, as the broad peak shown in Fig. 4B and C.

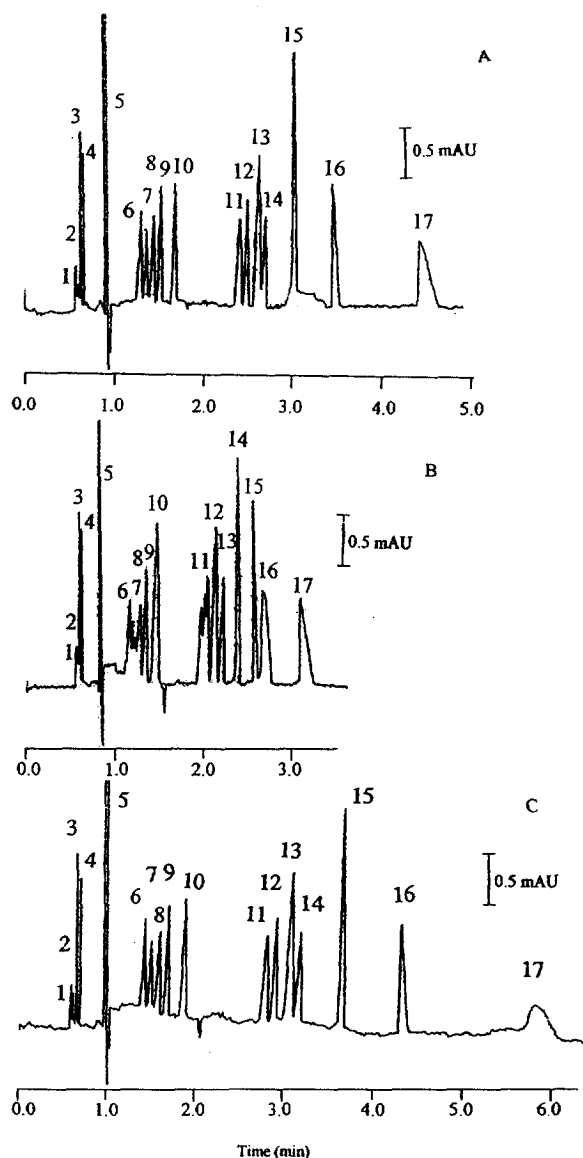


Fig. 3. Separation of four cations and twelve anions in the electrophoretic medium of 1,2-dimethylimidazole–trimellitic acid binary BGE under the optimal conditions as given in Table 3. (A) conditions of Case 1; (B) conditions of Case 2; (C) conditions of Case 3. Peak identification (all in $\mu\text{g/ml}$): 1= NH_4^+ (25.3), 2= K^+ (35.9), 3= Na^+ (110.6), 4= Li^+ (8.7), 5= H_2O , 6=ascorbate (13.3), 7= sorbate (15.5), 8=benzoate (27.5), 9=lactate (10.1), 10=acetate (25.3), 11=succinate (8.4), 12=malate (8.2), 13=tartrate (20.4), 14=maleate (8.9), 15=malonate (8.5), 16= perchlorate (8.7), 17=oxalate (6.7); other conditions as in Fig. 1.

Table 4

Limit of detection of the cations and anions^a

Ion	Limit of detection ($\mu\text{g/ml}$)
NH_4^+	2.0
K^+	5.0
Na^+	3.0
Li^+	0.5
Ascorbate	0.4
Sorbate	0.2
Benzoate	0.1
Lactate	0.09
Acetate	0.08
Succinate	0.2
Malate	0.2
Tartrate	0.2
Maleate	0.2
Malonate	0.2
ClO_4^-	0.6
Oxalate	1.0

^a The limits of detection for the ions were determined in the binary BGE: 1,2-dimethylimidazole=4.0 mM, trimellitic acid=0.90 mM, 18-crown-6=2.5 mM; pH=7.6; 3 times *S/N* criterion; other conditions as that in Fig. 1.

When the concentration of citrate exceeded that of the free hydrogen ion in the BGE under a certain pH condition, the excess citrate could be visualized as an individual zone superimposed on the broad peak. This explanation was confirmed by the fact that citrate could not be detected as a sharp peak when the orange juice was further diluted to 1:160, but it could be detected as a sharp peak when 21 $\mu\text{g/ml}$ citrate was spiked into this orange juice sample. Table 5 shows the concentration levels of some of the ions in the three soft drinks. By providing complete information of the cations and anions in soft drinks, the present method provides a useful procedure for monitoring the quality of these products and enable consumers to make better choices in selecting healthy foods.

4. Conclusion

The newly developed method is a simple approach for simultaneous separation and detection of alkali metals and organic acids. The proper selection of the components and detection wavelengths of the binary BGE is essential for the successful analysis of these two types of charged substances simultaneously.

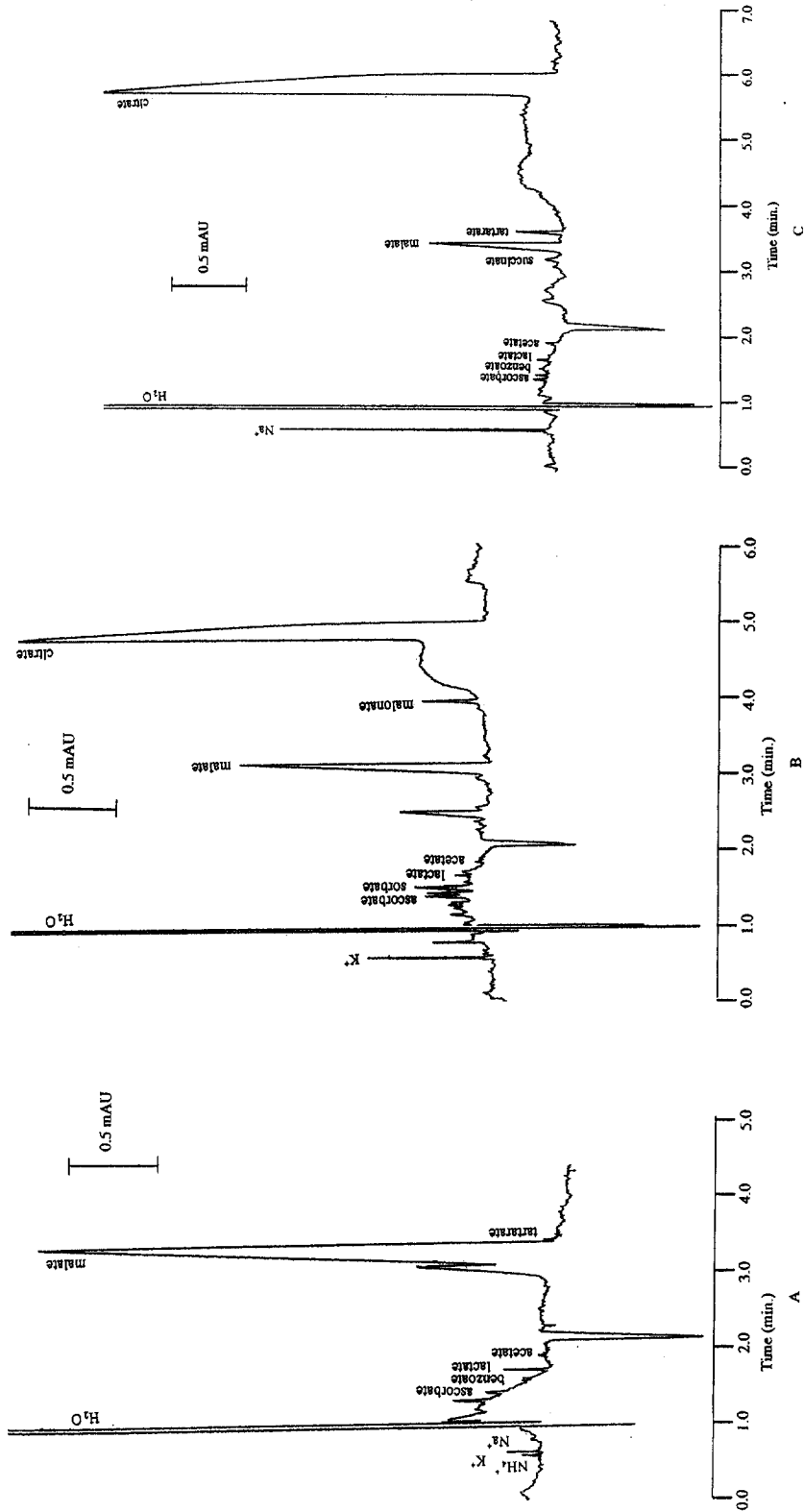


Fig. 4. Separation of three soft drinks in the 1,2-dimethylimidazole-trimellitic acid-18-crown-6 binary BGE under the optimal condition as given in the caption of Fig. 3C. (A) Apple juice, dilution 1:25; injection = 20 s; (B) orange juice, dilution 1:80; injection = 15 s; (C) grape juice, dilution 1:50; injection = 20 s; other conditions as in Fig. 3.

Table 5
Concentrations of selected ions in the three soft drinks

Ion	Content levels ($\mu\text{g}/\text{ml}$) ^a		
	Apple	Orange	Grape
K ⁺	244	2552	– ^b
Na ⁺	144	128	5200
Malate	1920	1010	278
Tartrate	12	– ^b	94
Malonate	– ^b	65	– ^b

^a The results were obtained under the conditions given in Fig. 2 with reproducibility (with respect to the measurement of peak height) of 2–8% R.S.D.. Dilution of the samples ranged from 1:10 to 1:100. The recovery of the ions determined ranged from 81 to 102%.

^b Ions could not be detected under the present conditions.

Cationic co-ions with higher pK_a values ($pK_a > 8$) should be used to compose this type of BGE because a wide working pH range could be achieved by using them and they could still function as co-ions of the cationic analytes at higher pH ($\text{pH} > 7$) conditions. The anionic co-ion should have similar mobility with those of the anionic analytes and comparable UV absorption with that of the cationic co-ion used to formulate the binary BGE in the selected UV absorption region; otherwise, masking of the UV absorption between the two components of the BGE would lead to the appearance of positive peaks (UV absorption of the sample zones was higher than background) and complex electropherograms. The fitted second-degree polynomial models with regard to the combined responses predict effectively the optimal conditions of the separation. This simplified optimization procedure could satisfy many separation requirements in practical analyses. The results obtained showed that the present method could be used in the analysis of real samples. It is more convenient than the individual separation approach and much more information could be obtained in a single run.

Acknowledgements

Financial support from the National University of Singapore is greatly appreciated.

References

- [1] R. Matissek, R. Wittkowski (Eds.), *High-performance Liquid Chromatography in Food Control and Research*, Technomic Publishing, Lancaster, PA, 1993.
- [2] O.A. Shpigun, Yu.A. Zolotov, *Ion Chromatography in Water Analysis*, Ellis Horwood, Chichester, 1988, p. 171.
- [3] S. F.Y. Li, *Capillary Electrophoresis (Journal of Chromatography Library, Vol. 52)*, Elsevier, Amsterdam, 1992.
- [4] J.W. Jorgenson, K.D. Lukacs, *Anal. Chem.* 53 (1981) 1298.
- [5] S.A. Shamsi, N.D. Danielson, *Anal. Chem.* 67 (1995) 4210.
- [6] F. Foret, S. Fanali, L. Ossicini, P. Bocek, *J. Chromatogr.* 470 (1989) 299.
- [7] K. Bachmann, I. Haumann, T. Groh, *Fresenius J. Anal. Chem.* 343 (1992) 901.
- [8] P. Kuban, B. Karlberg, *Anal. Chem.* 70 (1998) 360.
- [9] N. Avdalovic, C.A. Pohl, R.D. Rocklin, J.R. Stillian, *Anal. Chem.* 65 (1993) 1470.
- [10] X. Huang, J.A. Luckey, M.J. Gordon, R.N. Zare, *Anal. Chem.* 61 (1989) 766.
- [11] T. Soga, G.A. Ross, *J. Chromatogr. A* 767 (1997) 223.
- [12] Q. Yang, M. Jimidar, T.P. hamoir, J. Smeyers-Verbeke, D.L. Massart, *J. Chromatogr. A* 673 (1994) 275.
- [13] S.P.D. Lalljie, J. Vindevogel, P. Sandra, *J. Chromatogr. A* 652 (1993) 563.
- [14] W. Buchberger, S.M. Cousine, P.R. Haddad, *Trends Anal. Chem.* 13 (1994) 313.
- [15] S.M. Cousins, P.R. Haddad, W. Buchberger, *J. Chromatogr. A* 671 (1994) 397.
- [16] J.A. Dean (Ed.), *Lange's Handbook of Chemistry*, McGraw-Hill, New York, 1985.
- [17] R.M. Smith, A.E. Martell (Eds.), *Critical Stability Constants*, Vol. 6, 2nd supplement, Plenum Press, New York, 1989, p. 250.
- [18] A.E. Martell, R.D. Hancock, *Metal Complexes in Aqueous Solutions*, Plenum Press, New York, 1996, p. 212.
- [19] J.L. Beckers, *J. Chromatogr. A* 679 (1994) 153.
- [20] X. Xiong, S.F.Y. Li, *Electrophoresis*, 19 (1998) in press.
- [21] J.M. Riviello, M.P. Harrold, *J. Chromatogr. A* 652 (1993) 385.
- [22] M. Jimidar, B. Bourguignon, D.L. Massart, *J. Chromatogr. A* 740 (1996) 109.
- [23] J.C. Berridge, *Techniques for the Automated Optimization of HPLC Separation*, Wiley, Chichester, 1985, p. 21–25.
- [24] M.D. Valle, J. Alonso, M. Poch, J. Bartroli, *J. Chemom.* 3 (1988) 285.
- [25] A. Weston, P.R. Brown, *J. Chromatogr. A* 602 (1992) 249.
- [26] S.A. Shamsi, N.D. Danielson, *Anal. Chem.* 66 (1994) 3757.